Available online at www.sciencedirect.com
SCIENCE DIRECT®
Applied Numerical Mathematics 49 (2004) 415–430
APPLIED NUMERICAL MATHEMATICS
www.elsevier.com/locate/apnum

Non-equivalent partitions of d-triangles with Steiner points

Ángel Plaza [a,*], José P. Suárez [b], Miguel A. Padrón [c]

[a] *Department of Mathematics, University of Las Palmas de Gran Canaria, 35017, Spain*
[b] *Department of Cartography and Graphic Engineering, University of Las Palmas de Gran Canaria, 35017, Spain*
[c] *Department of Civil Engineering, University of Las Palmas de Gran Canaria, 35017, Spain*

Abstract

In this paper we present lower and upper bounds for the number of equivalence classes of d-triangles with additional or Steiner points. We also study the number of possible partitions that may appear by bisecting a tetrahedron with Steiner points at the midpoints of its edges. This problem arises, for example, when refining a 3D triangulation by bisecting the tetrahedra. To begin with, we look at the analogous 2D case, and then the 1-irregular tetrahedra (tetrahedra with at most one Steiner point on each edge) are classified into equivalence classes, and each element of the class is subdivided into several non-equivalent bisection-based partitions which are also studied. Finally, as an example of the application of refinement and coarsening of 3D bisection-based algorithms, a simulation evolution problem is shown.

Keywords: Steiner points; Triangulation; Bisection

1. Introduction

The number of different 1-irregular cuboids (cuboids with at most one additional point or *Steiner point* on each edge) that may appear when meshes are generated using extensions of the modified octree approach has recently been studied by Hitschfeld et al. [3]. Their paper is based on the modified octree approach to the mesh generation problem [16,15]. As is well known, in the modified octree method, the 3D domain is enclosed in a cube whose octants are repeatedly refined at their edge midpoints until the boundary and internal quantities are sufficiently approximated. The elements are then partitioned into tetrahedra. In this paper, we present a study of the number of partitions of 1-irregular d-triangles with Steiner (or additional) points at the midpoint edges. These 1-irregular d-triangles appear when studying

* Corresponding author.
E-mail address: aplaza@dma.ulpgc.es (Á. Plaza).

0168-9274/$30.00
doi:10.1016/j.apnum.2003.12.017

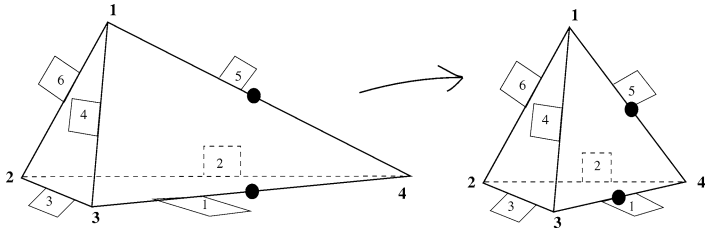

Fig. 1. Affine map from an irregular tetrahedron into an equilateral reference tetrahedron.

bisection-based refinement algorithms of triangular meshes in two and three dimensions, and could also be generalized to higher dimensions [6,7]. The use of pre-computed partitions as a method for finding the tessellation of any 1-irregular element is relevant when determining the final local triangulation. Furthermore, the correct partition is always computed and takes less computational time than a real time algorithm without this pre-computed calculations. Also, once the set of 1-irregular elements has been obtained, the application of a suitable partition to each 1-irregular element can easily be parallelized.

For local adaptive refinement, triangles and tetrahedra have been used and several bisection-based algorithms in two [4,11–14] and three [1,6,7] dimensions have been presented in recent years. The refinement of a triangular mesh can comprise two separate steps: firstly, the subdivision of the edges involved in the refinement while conformity is assured, and secondly, the subdivision of the involved triangles in two dimensions, or triangles and tetrahedra in three dimensions. In this sense, we can say that these algorithms are skeleton-based since they work on the hierarchy of the k-skeletons of the triangulation, the sets of k-faces for k between 1 and d. It should be noted that, in this way, adjacency relations are relevant for the first step, and for the second, we must consider the suitable set of partition patterns for the triangles (and tetrahedra) in which at least one edge has previously been divided. From now on we will refer to the elements in which there is at most one Steiner point on each edge as 1-irregular. Likewise, the elements in which at least one edge has been previously divided will be referred to as non-trivial 1-irregular elements.

As we are mainly interested in the relative positions of Steiner points we consider an affine transformation for mapping any given 1-irregular non-equilateral tetrahedron into an equilateral reference tetrahedron as shown in Fig. 1. Therefore, equilateral elements with Steiner points will be referred to as 1-irregular configurations.

The paper is organized as follows. In Section 2 we provide some basic definitions. In Section 3, 1-irregular d-triangles and equivalence classes or pattern types are studied. Following this, the number of partitions of the equivalence classes based on bisection is given. Then, in Section 5, we focus on the 3D 8-tetrahedra longest-edge partition. A numerical example showing the utility of bisection-based partition for mesh refinement is given in Section 6, and we finish off with some conclusions in Section 7.

2. Basic definitions

Definition 1. A d-triangle is the notation for a triangle (or simplex) of dimension d: a 0-triangle is a point, a 1-triangle is a segment, a 2-triangle is a triangle (default) and a 3-triangle is a tetrahedron. A d-triangle

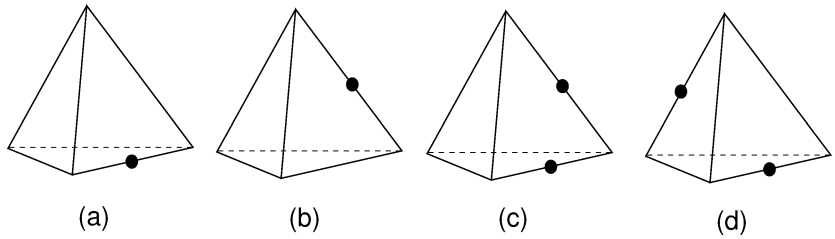

Fig. 2. Different 1-irregular configurations in tetrahedra.

can be also defined as the closed subset $T \subset \mathbb{R}^n$, $0 \leqslant d \leqslant n$ given by the convex linear hull of $d+1$ vertices $x_1, x_2, \ldots, x_{d+1}$ in $\mathbb{R}^n$:

$$T = [x_1, x_2, \ldots, x_{d+1}] = \left\{ x = \sum_{i=1}^{d+1} \lambda_i x_i \;\middle|\; \sum_{i=1}^{d+1} \lambda_i = 1;\ 0 \leqslant \lambda_i \leqslant 1,\ 1 \leqslant i \leqslant d+1 \right\}.$$

Definition 2. A triangulation T of a bounded set Ω with polygonal boundary is a partition of Ω into a set of triangles $T = \{t_1, t_2, \ldots, t_n\}$ such that $\Omega = \bigcup_{i=1}^{n} t_i$, $\operatorname{int}(t_i) \neq \emptyset$ for all i, $\operatorname{int}(t_i) \cap \operatorname{int}(t_j) = \emptyset$ if $i \neq j$, and $t_i \cap t_j$ if not empty is a common vertex, or a common edge (or in three dimensions it can also be a common face).

This last condition is frequently referred to as the conformity condition and is usually required in finite element codes.

1-irregular configurations in 3D are said to be the tetrahedra in which at most one Steiner point in an edge appears. The configuration with no Steiner points is called trivial configuration.

In order to consider equivalence classes in the set of 1-irregular configurations of d-triangles any 1-irregular d-triangle will be transformed firstly by an affine map into a reference 1-irregular equilateral d-triangle (see Fig. 1). Following [3] the next definition introduces the concept of equivalence class and pattern type.

Definition 3. Let c_1 and c_2 be two 1-irregular configurations, c_1 and c_2 belong to the same equivalence class if c_1 can be transformed to c_2 through rotations or reflections. The representative element of an equivalence class is called pattern type.

Fig. 2 shows several 1-irregular tetrahedra. The 1-irregular tetrahedron of Fig. 2(a) can be transformed into the 1-irregular tetrahedron of Fig. 2(b) by rotating it properly. We say, therefore, that the 1-irregular tetrahedra of Figs. 2(a) and (b) belong to the same equivalence class. The two 1-irregular tetrahedra of Figs. 2(c) and (d), respectively have two bisected edges but they do not belong to the same equivalence class.

1-irregular configurations belonging to the same equivalence class are subdivided into several non-equivalent bisection-based partitions. We should note that each pattern type has a bounded number of possible bisection-based partitions depending on the order in which the edges with Steiner points are taken for bisecting. In some longest-edge refinement algorithms in 2D [4,11–13] and in 3D [1,6,7] the edges are bisected by following the longest edge of each triangular face. Fig. 3 shows a 1-irregular triangle where different partitions appear depending on which is the longest edge.

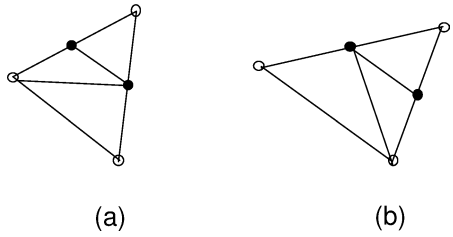

Fig. 3. The partition of a 1-irregular triangle with 2 Steiner points depends on the length of the bisected edges.

3. 1-irregular triangles and equivalence classes using a bisection based approach

The number of 1-irregular triangles is 2^3 in 2D, and 2^6 in 3D. However, the number of equivalence classes or pattern types is much lower than the total number of 1-irregular configurations as we will show in this section. Some generic dimension study is given here, although we are mainly interested in 2 and 3 dimensions.

3.1. Theoretical lower bounds

Theorem 4. *A d-triangle* (*d-simplex*) *has* $d+1$ *vertices and* $\binom{d+1}{2} = \frac{(d+1)d}{2}$ *edges. In general, a d-triangle has* $\binom{d+1}{k+1} = \frac{(d+1)d(d-1)\cdots(d-k+1)}{(k+1)!}$ *k-faces, that is, faces of dimension k.*

Theorem 5. *Let t be a d-triangle. The number of* 1*-irregular configurations of t is* $2^{\binom{d+1}{2}} = 2^{\frac{(d+1)d}{2}}$.

Proof. Each edge of the d-triangle may or may not be bisected. Thus, there are two possibilities for each edge (to have one or no Steiner point) and there are $2^{\text{number-of-edges}}$ possible 1-irregular configurations. In this way, a d-triangle has $2^{\binom{d+1}{2}} = 2^{\frac{(d+1)d}{2}}$ 1-irregular configurations. □

Corollary 6. *The total number of* 1*-irregular configurations is an upper bound of the number of equivalence classes.*

Theorem 7. *A lower bound for the number of equivalence classes of a d-triangle is* $\max\{\binom{d+1}{2}, \lceil 2^{\binom{d+1}{2}-d-\log_2(d+1)d} \rceil\}$.

Proof. Note first that the number of edges in a d-triangle, $\binom{d+1}{2}$, is a lower bound for the number of equivalence classes. Following the same argument here as [3] we have to consider that all the rotations and reflections are useful to identify two configurations under equivalence. Then:

(1) Each reflection divides the set of 1-irregular configurations into two parts. Any reflection which takes a regular tetrahedron into itself necessarily takes a cube into itself, but not vice versa [2], see Fig. 4. There are d reflections for a d-dimensional cube and therefore the reduction factor obtainable using reflections is at most 2^d.
(2) Using rotations, it is possible to bring any edge to a fixed edge. Furthermore, it is possible to choose two orientations. Thus, the reduction factor obtainable through rotations is at most $d(d+1)$.

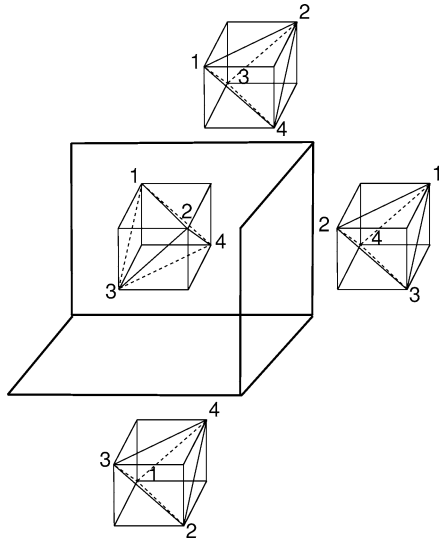

Fig. 4. Tetrahedron inscribed in cube and possible reflections.

Table 1
Evolution of lower bounds for 1-irregular configurations

d	$s1$	$s2$	Lower-bound
1	1	1	1
2	3	1	3
3	6	1	6
4	10	4	10
5	15	35	35
6	21	781	781
7	28	3.7449×10^4	3.7449×10^4
8	36	3.7283×10^6	3.7283×10^6
9	45	7.6355×10^8	7.6355×10^8
10	55	3.1986×10^{11}	3.1986×10^{11}

In the best case the 1-irregular configurations obtainable using reflections and rotations are distinct. Thus, the reduction factor is at most $2^d d(d+1)$, and a lower bound for the number of configurations is:

$$\left\lceil \frac{2^{\binom{d+1}{2}}}{2^d \cdot d(d+1)} \right\rceil = \left\lceil 2^{\binom{d+1}{2} - d - \log_2 (d+1)d} \right\rceil \qquad \square \tag{1}$$

The evolution of lower bounds proposed by the previous theorem for the first dimensions d is shown in Table 1, in which $s1 = \binom{d+1}{2}$, $s2 = \lceil 2^{\binom{d+1}{2} - d - \log_2 (d+1)d} \rceil$. Note that for low dimensions $s2$ is negligible, but for $d \geqslant 4$, is meaningful.

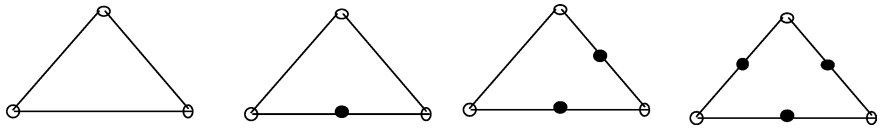

Fig. 5. Pattern types in 2D.

3.2. Exhaustively counting in two and in three dimensions

We will now study the number of non-equivalent configurations that appear by means of Steiner edge midpoints in two and three dimensions.

Theorem 8. *The number of non-equivalent configurations or pattern types in* 2D *is* 4 (*see Fig.* 5), *and the number of possible configurations is* 8.

In order to calculate the number of equivalence classes for the 3D case, an algorithm computing which configurations are equivalent is given below. For each possible configuration, it performs all the possible combinations of rotations and reflections. Each 1-irregular configuration is represented by a set of the edges with Steiner points, for example, $\{1, 2\}$ means the configuration in which edges 1 and 2 have Steiner points. Therefore the set of all 1-irregular configurations can be identified with the set of parts of $\{1, 2, \ldots, 6\}$.

Algorithm I.

/* Input variable: S, set of all 1-irregular configurations
/* Output variable: Q, set of pattern types
$Q = \{\emptyset\}$
While $S \neq \{\emptyset\}$ **do**
    Let $s_i \in S$
    Perform rotations and reflections on s_i
    Let $R(s_i)$ be the set of configurations equivalent to s_i
        through rotations and reflections
    $S = S - \{s_i \cup R(s_i)\}$
    $Q = Q \cup \{s_i\}$
End While

After applying this algorithm all the pattern types are obtained. This algorithm can be used to automatically generate the corner permutation between any configuration and its pattern type, and hence, to identify the right partition in O(1).

Table 2 shows the possible rotations for a standard tetrahedron in which edges have been labelled as in Fig. 6. The first column in the table represents the rotation applied: *axis* stands for one of the two possible axes to rotate the tetrahedron, as in Fig. 6, and *angle* is the involved angle for the rotation in degrees. Column two represents the cycles of edges in the rotations, for instance, (16) means that edge 1 is moved

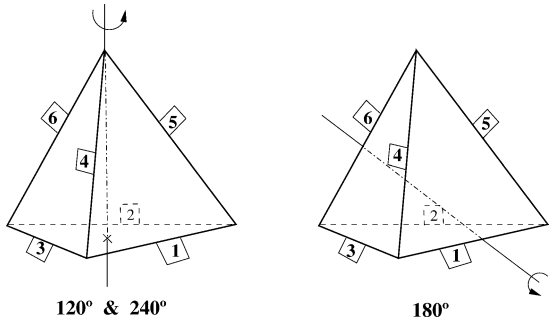

Fig. 6. Rotations of a tetrahedron.

Table 2
Rotations to the standard tetrahedron

rot(axis, angle)	Edge permutations
rot(∅, ∅)	(1)(2)(3)(4)(5)(6)
rot(axis1, 120°)	(123)(456)
rot(axis2, 240°)	(145)(362)
rot(axis3, 120°)	(256)(143)
rot(axis4, 240°)	(364)(125)
rot(axis1, 240°)	(132)(465)
rot(axis2, 120°)	(154)(326)
rot(axis3, 240°)	(265)(134)
rot(axis4, 120°)	(346)(152)
rot(axis1-6, 180°)	(1)(24)(35)(6)
rot(axis2-4, 180°)	(2)(16)(35)(4)
rot(axis3-5, 180°)	(3)(16)(24)(5)

to edge 6, and vice versa. Since the edges are represented by labels, a simple bits-like operation of left shift on the label cycle is performed for the corresponding rotation.

Theorem 9. *There are* 12 *equivalence classes of* 1*-irregular configurations in* 3D.

Proof. It is known that the group of isometries for the tetrahedron has 12 elements, $|G| = 12$. These elements are the following: identity, which is denoted as $(1)(2)(3)(4)(5)(6)$; then for each fixed vertex we can consider a rotation of 120° or a rotation of 240°. These rotations, the product of cycles, are denoted as: $(1, 2, 3)(4, 5, 6)$, and $(1, 3, 2)(4, 6, 5)$, respectively. Considering that there are 3 more vertices to take these rotations, 8 movements are counted.

Finally, a rotation of 180° can be considered if the line passing through the midpoints of two opposite edges is taken as the rotation axis. One of these rotations can be denoted as $(1)(2, 4)(3, 5)(6)$ since the two opposite edges are invariant under this rotation and the other opposite edges change with the one opposite them. There are three pairs of opposite edges so we have 3 of these rotations.

Following Algorithm I, 12 equivalence classes of 1-irregular configurations of tetrahedra are obtained. These 12 different configurations are shown in Fig. 7. □

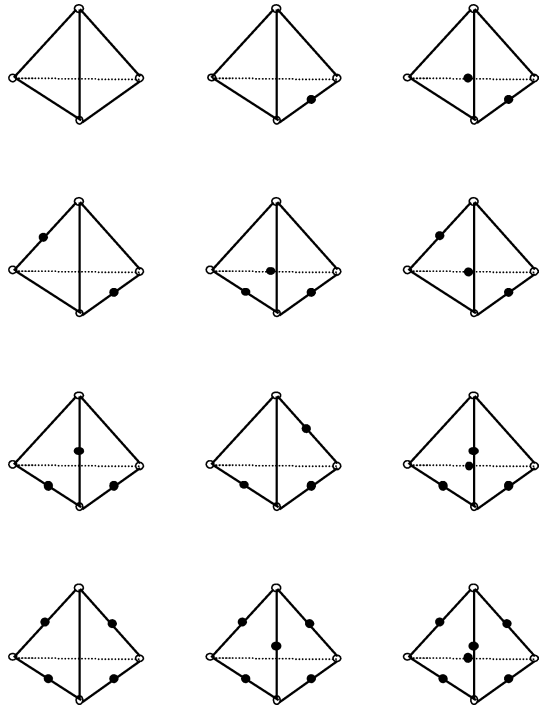

Fig. 7. The 12 non-equivalent configurations for a tetrahedron.

4. Number of bisection-based partitions for pattern types

We will now give some bounds for the number of possible bisection-based partitions of a d-triangle with Steiner points. Note that the number of partitions depends not only on the number of Steiner points on the midpoint edges of the d-triangle, but also on the order in which the bisected edges are taken for successive bisections.

Theorem 10. *The number of bisection-based partitions for each d-triangle is bounded by*:

$$F(d) = \sum_{k=0}^{\binom{d+1}{2}} \binom{\binom{d+1}{2}}{k} \cdot k!.$$

Proof. As we have noted before, for a particular 1-irregular tetrahedron different partitions can be obtained by taking the edges with Steiner points in a different order. Since the number of different orders of k objects is $k!$, this leads us to a bound in the number of possible partitions of a triangle with k Steiner points as $\binom{\binom{d+1}{2}}{k} \cdot k!$, and taking the sum in the index k we get the formula. □

Note that for dimension $d \leqslant 3$, $F(d)$ is not too high, but for $d \geqslant 4$, $F(d)$ is extremely high. This is due to the factor $k!$ in the formula. Note that the partitions we are considering are based on bisection and the order of bisection is not always the key to obtaining different partitions. Previous bounds can be improved as the following theorem establishes.

Table 3
Behavior of $F(d)$ and $G(d)$

d	$F(d)$	$G(d)$
1	2	2
2	16	12
3	1 957	284
4	9 864 101	21 173
5	3 554 627 472 076	3 999 676
6	138 879 579 704 209 680 022	627 715 222

Theorem 11. *The number of bisection based partitions for each d-triangle is bounded by*:

$$G(d) = \sum_{k=0}^{\binom{d+1}{2}} \binom{\binom{d+1}{2}}{k} \cdot \min(d,k)!.$$

Proof. Here we consider that after at most d bisections of the d-triangle $k-d$ edges remain to be bisected but all of them are in different sub-triangles, and so the order in which these last edges are taken is irrelevant for the number of distinct partitions. □

Table 3 shows the values of $F(d)$ and $G(d)$ for each dimension d.

5. The 3-dimensional case: The 8T-LE partition

In three dimensions the number of different possible partitions of tetrahedra based on bisection has been studied by Plaza and Carey in [6] in the context of the skeleton-based refinement (SBR) algorithm. They obtain 51 different non-trivial partitions. Also in [9] previous bound has been reduced to 30 partitions considering reflections. In Fig. 12 all these non-trivial different partitions of a tetrahedron are shown.

The 3D-SBR algorithm generalizes the 4 triangles longest-edge refinement algorithm of Rivara [11, 12], to 3 dimensions. The 3D-SBR algorithm uses partitions in eight tetrahedra for those elements to be refined. The following 8-tetrahedra longest-edge partition was introduced and discussed by Plaza and co-authors [5–10].

Definition 12 (*The* 8*-tetrahedra longest-edge* (8*T-LE*) *partition*). For any tetrahedron t the 8T-LE partition of t is obtained as follows:

(1) Longest edge bisection of t producing tetrahedra t_1, t_2.
(2) Bisection of t_i, for $i = 1, 2$, by the longest edge of the common face of t_i with the original tetrahedron t, producing tetrahedra t_{ij}, for $j = 1, 2$.
(3) Bisection of each t_{ij} by the midpoint of the unique edge equal to an edge of the original tetrahedron.

Note that for a local refinement of a 3D triangulation we should consider not only the 8T-LE partition of a single tetrahedron, but also the set of partial bisection-based divisions of 1-irregular tetrahedra. These

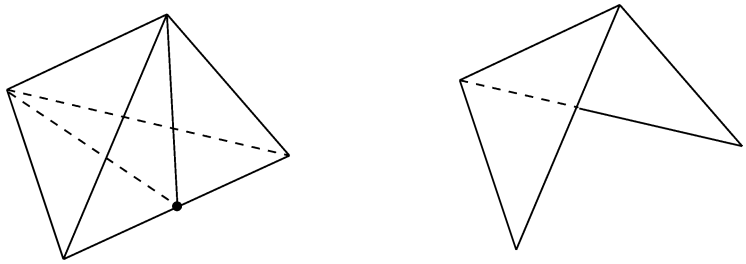

Fig. 8. The simple division for a tetrahedron and its secondary faces.

partial bisection-based divisions are determined by the longest edges of the faces of the tetrahedra, and through the suitable identification in equivalence classes by the relative positions of the longest edges of the faces.

5.1. Classification of the tetrahedra

Let us consider a generic tetrahedron. We can label edges as in Fig. 1 so that edge 1 is the longest. The faces are labelled with the number of the opposite vertex, as always. We assign a *type*-label, 1, 2, or 3 to each edge of a tetrahedron: the longest edge of a tetrahedron is labelled *type* 1. Note that this edge is also the longest edge of two faces (1 and 2) which share this edge. The longest edge of each of the other two faces is edge *type* 2, and the rest of the edges are *type* 3. Edge *type* 1 is the reference edge of the tetrahedron.

Theorem 13. *For a tetrahedron there are* 90 *possible bisection-based partitions including the no division.*

Proof. We should point out that each different possible bisection-based partition obtained by simple bisection is fixed by the number and relative position of the nodes introduced at the midpoints of the edges. These nodes, out of the midpoint node at the longest edge of the tetrahedron, appear on faces 4 and 3. In other words, to know the number of possible bisection-based partitions by bisection of a tetrahedron, we have to know the possible divisions for faces 3 and 4 and add two more: the simple bisection and the no bisection cases.

There are only 4 possible divisions of a triangular face if we know the longest edge. *A priori* for faces 3 and 4, the longest edge can be any of the edges, so there are $3 \times 4 = 12$ different possible divisions for each triangular face, and taking into account the no division of faces 3 and 4, we get 13 possibilities. Faces 3 and 4 share edge 6. If edge 6 is divided, 8 cases can be distinguished, as are shown in Fig. 9. Otherwise, if edge 6 has not been divided, 5 cases appear (see Fig. 10). The total number of bisection-based partitions is shown in the next table:

Edge 6 divided	$8 \times 8 =$	64
Edge 6 no divided	$5 \times 5 =$	25
No division		1
TOTAL		90

Nevertheless, many of the 90 bisection-based partitions are equivalent through rotation.

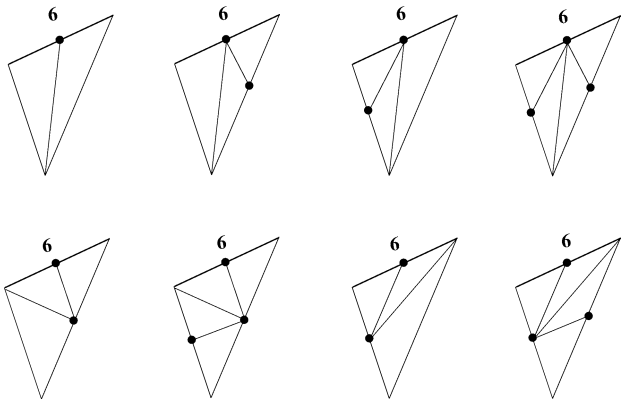

Fig. 9. Eight possibilities if edge 6 is subdivided.

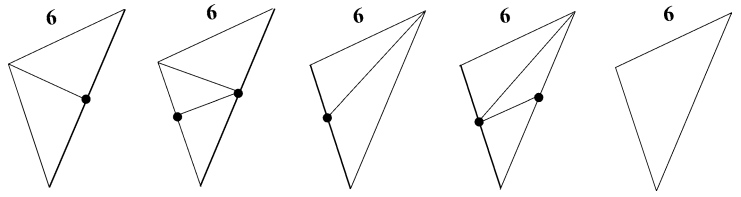

Fig. 10. Five possibilities if edge 6 is not subdivided.

We distinguish three types of tetrahedra based on the relative position of their edge-types. We consider the subdivision of the tetrahedra in order, according to their edge-type: first, the tetrahedron bisected by the longest edge, secondly by edges type 2, and so on.

Procedure Classification (t)
If edge 6 has type 3, **then**
  t has type 1
Else if edge 6 = longest(face3) = longest(face4) **then**
  t has type 2
Else
  t has type 3
End if

Note that the simplest bisection-based partition obtained by *local* refinement is that in which only one node is introduced at the midpoint of the longest edge of the tetrahedron. We will denote this configuration as (1). *Global* refinement of a tetrahedron means that a node has been introduced in each one of its edges. We begin by pointing out the equivalence of the possible configurations that are obtained by pure rotation. Let the tetrahedron of Fig. 11 be rotated by π radians on an axis through the midpoints of edges 1 and 6. Again we obtain the tetrahedron in canonical position, but the local numeration of its edges has changed. If this rotation is denoted by r, the relations between the edges are: $r(1) = 1$; $r(2) = 4$; $r(3) = 5$; and $r(6) = 6$.

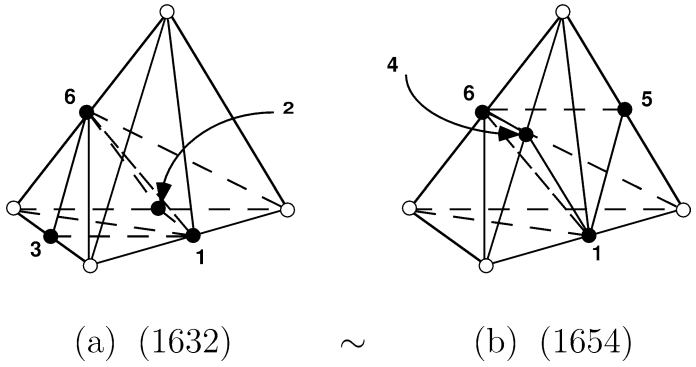

Fig. 11. Two equivalent bisection-based partitions under rotation.

Table 4
Possible non-trivial bisection-based partitions obtained by tetrahedron subdivision of "*na*" edges. Integer sequences in bold indicate distinct bisection-based partitions and # is the number of distinct (**bold**) bisection-based partitions in each case

na	Tet type 1	Tet type 2	Tet type 3	#
1	**(1)**	(1)	(1)	1
2	**(12)** ∼(14) **(13)**∼(15)	**(16)**	(12)∼(14) (13)∼(15)	3
3	**(125)**∼(143) **(134)**∼(152) **(123)**∼(145) **(124)** **(135)**	**(162)**∼(164) **(163)**∼(165)	(125)∼(143) (134)∼(152) **(126)**∼(146) **(136)**∼(156)	9
4	**(1236)**∼(1456) **(1234)**∼(1452) **(1235)**∼(1453) **(1356)** **(1354)**∼(1532) **(1426)** **(1423)**∼(1245)	**(1654)**∼(1632) **(1625)**∼(1643) **(1624)** **(1635)**	**(1265)**∼(1463) **(1364)**∼(1562) **(1263)**∼(1465) **(1264)**∼(1462) **(1362)**∼(1564) **(1365)**∼(1563)	17
5	**(12364)**∼(14562) **(12365)**∼(14563) **(12345)**∼(14523) **(12463)**∼(14265) **(13524)** **(13562)**∼(15364) **(14235)**	**(16234)**∼(16452) **(16235)**∼(16453)	**(12653)**∼(14635) **(12654)**∼(14632) **(13645)**∼(15623) **(13642)**∼(15624) **(12634)**∼(14652) **(13625)**∼(15643)	15
6	**(123456)**∼(145236) **(124356)** **(135246)**	**(162345)**	**(126345)**∼(146523) **(136245)**∼(156423)	6
#	25	10	16	**51**

Let us represent each bisection-based partition by means of integer sequences of the form $(i \dots l)$ where the number of edges that are subdivided are listed in order according to their types, from type 1 to type 3. For instance, the bisection-based partition of Fig. 11(a) is represented as (1623) since it is characterized by midpoint nodes of edges 1, 6, 2 and 3. (Here edge 6 is type 2, since it is the second in the sequence, and as it is opposite to the reference edge (1), the tetrahedron type 2 in which 4 nodes are added). For comparison, the bisection-based partition (1645) is shown in Fig. 11(b).

Let *IS* be the following set: $IS = \{\sigma$, such that $\sigma = (i_1, \dots, i_k)$, where $k \leqslant 6$, $i_j \in 1, 2, \dots, 6$, $i_1 = 1$ and $i_n \neq i_m$ if $n \neq m\}$. For a given rotation r and for $\sigma = (i_1, \dots, i_k) \in IS$, we define $r(\sigma) = (r(i_1), \dots, r(i_k))$.

For the sequences in *IS* of the same length we define an equivalence relation in this way:

(1) if $r(\sigma_1) = \sigma_2$, then $\sigma_1 \sim \sigma_2$;
(2) if $\sigma_1 = \sigma_2$ except for the order of edges with the same type, then $\sigma_1 \sim \sigma_2$.

Applying the equivalence relations given is sufficient so that all the possible bisection-based partitions are non-equivalent under rotations.

Theorem 14 [6,7]. *There are* 51 *different non-trivial possible bisection-based partitions, through rotations.*

Theorem 15 [9]. *There are exactly* 30 *different patterns* (*invariant under rotation, and reflection*) *associated with the partition of a tetrahedron.*

The 30 different patterns are shown in Fig. 12.

6. Numerical example

Here we present the simulation of a 3D singularity propagation problem by refining and coarsening an L-shaped domain using the 8T-LE partition. As the front moves across the domain, the tetrahedral grid is adaptively refined in the zone the front is invading, and derefined in the zone the front is vacating.

In Fig. 13 we show the Log of the number of tetrahedra vs. the number of refinements. The derefinement algorithm assures that the number of tetrahedra—and nodes—remains bounded throughout the entire process. Fig. 14 shows the evolution of meshes for this evolution problem. Only some of the most relevant refined meshes are shown in the figure. The combination refinement/derefinement allows us to obtain a very small refined zone and allows this refined area to change as the front moves.

7. Conclusions

The number of possible partitions that may appear by bisecting a tetrahedron with Steiner points at the midpoints of the edges has been studied. This problem is of greatest interest when refining a 3D tetrahedral triangulation by bisection. 1-irregular tetrahedra can be handled using a hash table, and therefore the refined triangulation can always be found in constant time. Moreover, some bounds for this problem in general dimension d have been provided here.

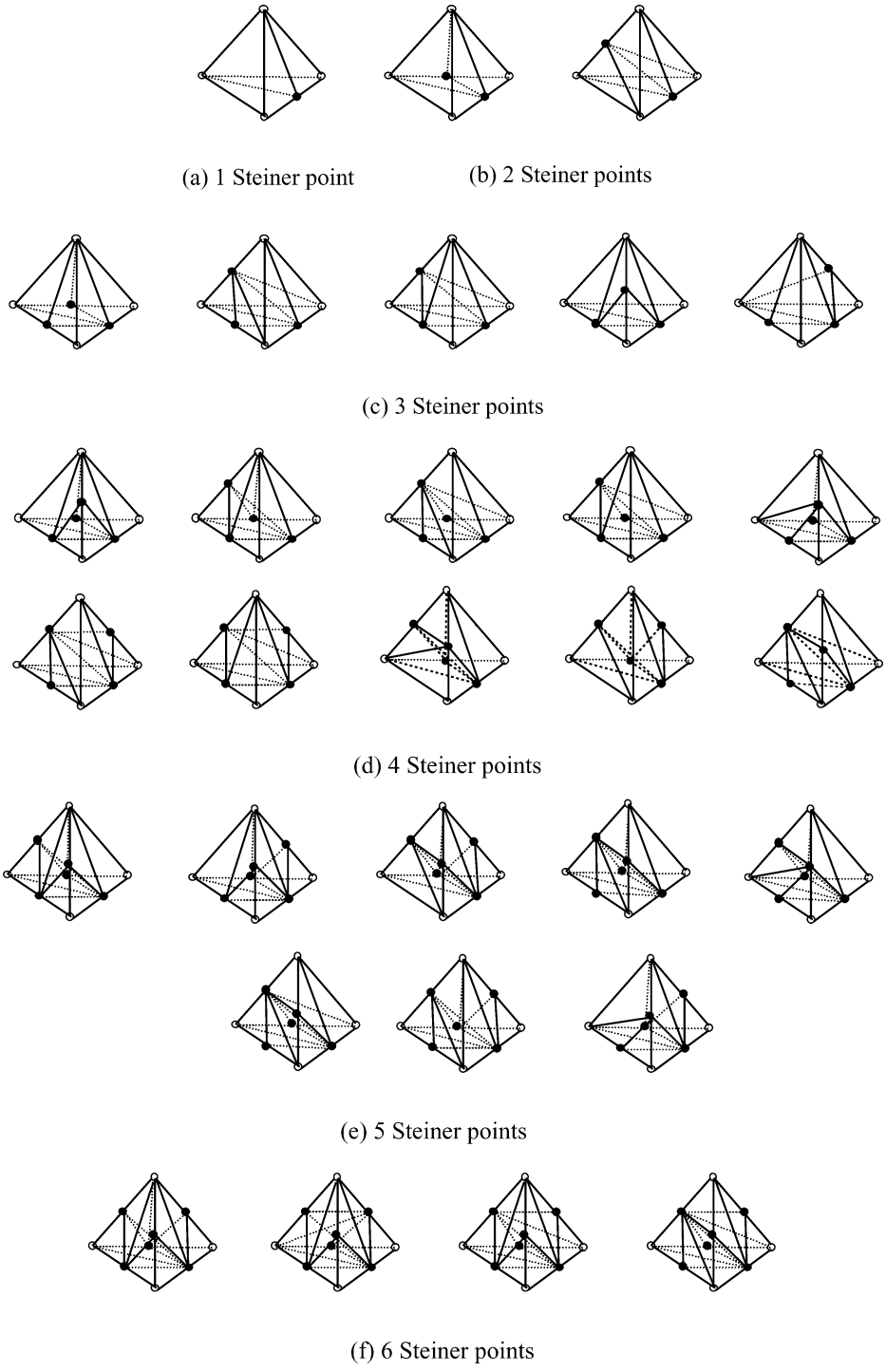

Fig. 12. The 30 non-equivalent non-trivial bisection-based partitions of a tetrahedron.

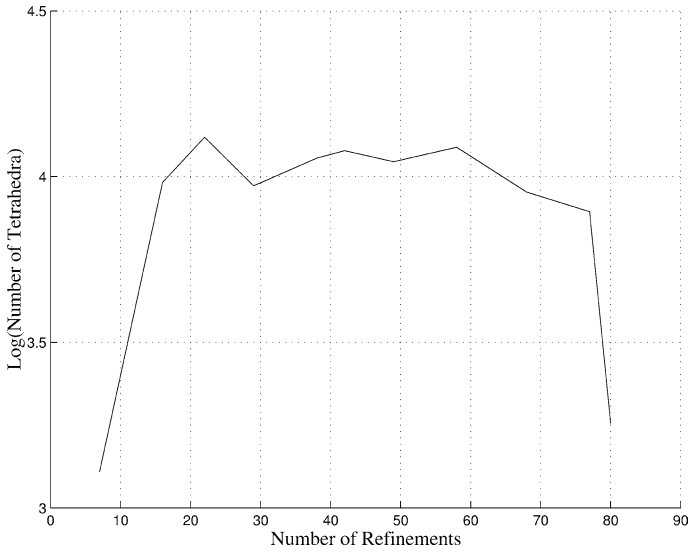

Fig. 13. Evolution of tetrahedra versus number of refinements.

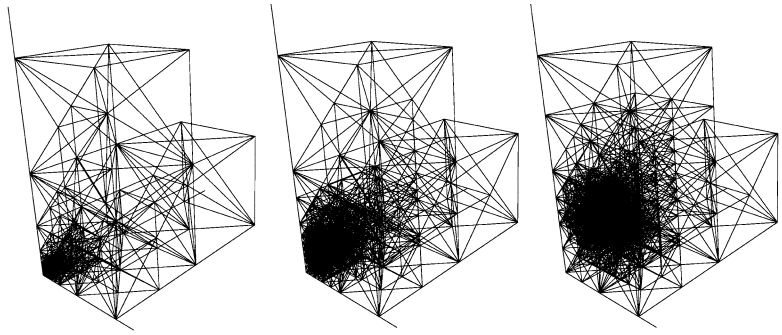

(a) 366 n. & 2472 t. (b) 1823 n. & 8611 t. (c) 1743 n. & 9380 t.

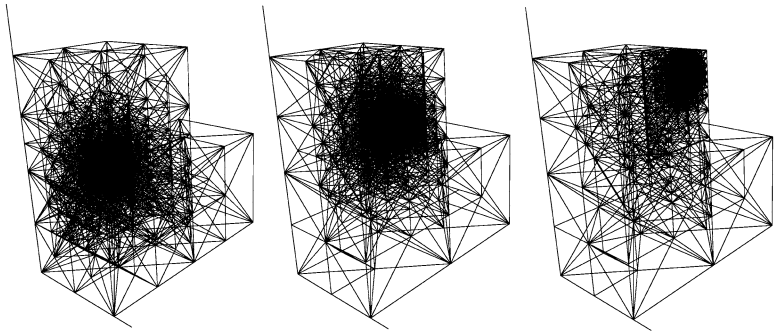

(d) 2175 n. & 11978 t. (e) 2254 n. & 12262 t. (f) 1515 n. & 7836 t.

Fig. 14. Simulation example in 3D dimensions of a punctual moving front.

The use of pre-computed partitions as a method for finding the tessellation of any 1-irregular element, which can be independent of the algorithm used to generate them, should be preferred over other methods, because it is a robust method. In addition to this, it always computes the correct partition and takes less computational time than a real time algorithm.

Acknowledgement

This work was supported in part by ULPGC Grant number UNI2002/22. We are also grateful to the referee for his helpful comments.

References

[1] E. Bänsch, Local mesh refinement in 2 and 3 dimensions, Impact Comput. Sci. Engrg. 3 (1991) 181–191.
[2] P.R. Cromwell, Polyhedra, Cambridge University Press, Cambridge, 1997.
[3] N. Hitschfeld, G. Navarro, R. Farías, Tesselations of cuboids with Steiner points, in: Proceedings of the 9th International Meshing Roundtable, New Orleans, Luoisiana, 2000, pp. 275–282.
[4] W.F. Mitchell, Optimal multilevel iterative methods for adaptive grids, SIAM J. Sci. Statist. Comput. 13 (1992) 146–167.
[5] M.A. Padrón, A 3D Derefinement Algorithm for Tetrahedral Nested Meshes Based on the Skeleton, Ph.D. Thesis, University of Las Palmas de Gran Canaria, 1999 (in Spanish).
[6] A. Plaza, G.F. Carey, About local refinement of tetrahedral grids based on bisection, in: 5th Inter. Mesh. Roundtable, Sandia Corporation, 1996, pp. 123–136.
[7] A. Plaza, G.F. Carey, Local refinement of simplicial grids based on the skeleton, Appl. Numer. Math. 32 (2) (2000) 195–218.
[8] A. Plaza, M.A. Padrón, G.F. Carey, A 3d refinement/derefinement combination for solving evolution problems, Appl. Numer. Math. 32 (4) (2000) 401–418.
[9] A. Plaza, M.C. Rivara, Mesh refinement/derefinement based on the 8-tetrahedra longest-edge partition, DCC-99-6 Technical Report, Dept. de CC. de la Computación, U. de Chile, 1999.
[10] A. Plaza, M.-C. Rivara, On the adjacencies of triangular meshes based on skeleton-regular partitions, J. Comput. Appl. Math. 140 (2002) 673–693.
[11] M.C. Rivara, Mesh refinement based on the generalized bisection of simplices, SIAM J. Numer. Anal. 2 (1984) 604–613.
[12] M.C. Rivara, A grid generator based on 4-triangles conforming mesh refinement algorithms, Internat. J. Numer. Methods Engrg. 24 (1987) 1343–1354.
[13] M.C. Rivara, Selective refinement/derefinement algorithm for sequences of nested triangulations, Internat. J. Numer. Methods Engrg. 28 (1989) 2889–2906.
[14] M.C. Rivara, New longest-edge algorithms for the refinement and/or improvement of unstructured triangulations, Internat. J. Numer. Methods Engrg. 40 (1997) 3313–3324.
[15] M.S. Shephard, M.K. Georges, Automatic three dimensional generation by the finite octree technique, Internat. J. Numer. Methods Engrg. 32 (1991) 709–749.
[16] M.A. Yerry, S. Shephard, Automatic three-dimensional mesh generation by the modified-octree technique, Internat. J. Numer. Methods Engrg. 20 (1984) 1965–1990.